

Solvent-free synthesis of carboxylate-functionalized cellulose from waste cotton fabrics for the removal of cationic dyes from aqueous solutions

Dong Tian · Xinxing Zhang · Canhui Lu ·
Guiping Yuan · Wei Zhang · Zehang Zhou

Received: 4 May 2013 / Accepted: 12 November 2013 / Published online: 17 November 2013
© Springer Science+Business Media Dordrecht 2013

Abstract In this work, the carboxylate-functionalized cellulose (CFC) from waste cotton fabrics (WCF) was studied for removal of cationic dyes from aqueous solutions. Instead of using conventional process for esterifying cellulose, which uses sulfuric or perchloric acid as catalysts, and methylene chloride as solvent, a novel mechanochemical approach which requires no catalyst or solvent in the reaction mixture was used. The prepared CFC with high concentrations of carboxyl groups ranging from 1.34 to 2.14 mmol/g was tested as adsorbent for the removal of methylene blue (MB) and rhodamine 6G (R6G) from aqueous solutions. The modified cellulose showed much higher adsorption capacity than that of unmodified WCF. The effect of operating variables such as concentration of carboxyl groups, solution pH, adsorbent dosage, temperature, and initial dye concentration on the adsorption capacity were investigated. The maximum adsorption capacity (185.63 mg/g for MB and 118.21 mg/g for R6G) was

obtained at pH = 10 and temperature of 298 K. The experimental equilibrium data were analyzed by using Langmuir and Freundlich isotherm models and the results indicated that the adsorption behavior of both dyes could be described well by Langmuir isotherm. The value of standard enthalpy changes was -26.48 kJ/mol for MB and -42.16 kJ/mol for R6G, suggesting that the adsorption process is exothermic in nature. The results revealed that solvent-free mechanochemistry is an environmentally friendly method to prepare novel efficient adsorbent for the removal of dyes from wastewater.

Keywords Carboxylate-functionalized cellulose · Waste cotton fabrics · Adsorbent · Mechanochemical · Acetylation · Cationic dye

Introduction

Organic dyes are widely used as coloring agents in a variety of industries, such as textiles, leather, paper, plastics, etc. It is estimated that more than 100,000 kinds of commercially available dyes with over 7×10^5 tonnes of dyestuff produced annually and 10–15 % of them lost in the effluent during the dyeing process (Demirbas 2009). As a result, a considerable amount of colored wastewater is produced, which brings about a severe public health concern and serious environmental problems. It should be noted

D. Tian · X. Zhang · C. Lu (✉) · W. Zhang · Z. Zhou
State Key Laboratory of Polymer Materials Engineering,
Polymer Research Institute of Sichuan University,
Chengdu 610065, China
e-mail: canhuilu@scu.edu.cn

G. Yuan (✉)
Analytic and Testing Center of Sichuan University,
Chengdu 610065, China
e-mail: ygp_04@163.com

that even a small quantity of dye in water (1.0 mg/L) can be highly visible, making it unfit for human consumption (Salleh et al. 2011). Colored wastewater can also affect the health of aquatic creatures. Thus an entire ecosystem can be destroyed by the contamination of various dyes in water. What is worse, some dyes are also toxic and even carcinogenic. For example, methylene blue (MB), commonly used as substance for dyeing cotton, wood and silk, can cause permanent injury to the eyes of human and animals. On inhalation, it can give rise to short periods of rapid or difficult breathing while ingestion through the mouth can produce a burning sensation and cause nausea, vomiting, profuse sweating, mental confusion and methemoglobinemia. Therefore, to protect humans and ecosystem from contamination, dyes should be removed from wastewater before being released into the environment (Mane et al. 2007).

Many available treatment processes such as coagulation, chemical oxidation, ultrasound oxidation and membrane-based separation are available for the treatment of dye-contained wastewater. However, they are not very successful due to many restrictions (Nandi et al. 2009). Liquid-phase adsorption has been proven to be an effective way and activated carbon is the most widely used adsorbent for the treatment of dye wastewater. However, its application is limited because of relatively high price and complex producing process (Saliba et al. 2002). Therefore, there is still a growing need in developing low-cost, renewable, locally available materials as adsorbent for the removal of dye from wastewater.

Over the last few decades, there has been an increase in the use of waste materials and by-products from agriculture and industry for dye removal from wastewater. The booming of the adsorption is due to its abundance in nature and less processing requirements. These researches focused on finding new low-cost adsorbents such as guava leaf powder (Ponnusami et al. 2008), tea waste (Uddin et al. 2009), princess tree leaf (Deniz and Saygideger 2011), cotton fiber (Mao et al. 2011), chitosan (Yang et al. 2013), etc. and studying the adsorption kinetics. However, raw waste materials or by-products have limited adsorption capacity due to their low accessibility (Annadurai et al. 2002; Bulut and Aydin 2006). Therefore, the modification of raw adsorbents to increase their removal efficiency is important. Rafatullaha et al. (2010) reviewed the use of low-cost adsorbents for the

removal of MB in his latest paper and strongly suggested that more work should be carried out in modification of the basic adsorbent medium.

Carboxylation and amination of raw adsorbents have been developed to improve their adsorption efficiency for dyes. Chao et al. (2004) developed an enzyme to graft carboxyl groups onto chitosan. As a result, the modified chitosan had the ability to adsorb both cationic and anionic dyes from wastewater. Gong et al. (2005) introduced three major functional groups (amino, carboxyl and hydroxyl groups) onto the peanut hull through solvent-based chemical methods and found that carboxyl group was the major functional group in the adsorption of cationic dyes. Xu et al. (2010) prepared a new adsorbent prepared by the reaction of wheat straw with epichlorohydrin and trimethylamine in the presence of ethylenediamine and N, N-dimethylformamide. Their results indicated that the modified wheat straw was capable of removing anionic dyes. However, these solvent-based chemical methods have some disadvantages such as the use of toxic organic solvents, complex preparation and high temperature processing.

Herein we present a simple and environmentally friendly method, solvent-free mechanochemistry, to prepare carboxylate-functionalized cellulose (CFC) from waste cotton fabrics (WCF). The modified cellulose can be used as a new low-cost and efficient adsorbent for the removal of cationic dyes from aqueous solutions. WCF is itself a kind of industrial wastes from cotton textile industry and can be easily obtained by paying the freight (no more than \$30 a tonne) in China. Generally, used clothes and leftover materials of textile industry end in waste stations are usually landfilled or incinerated (Miranda et al. 2007). These disposing methods not only create environmental pollution but also lead to great waste of the valuable resources. In our previous studies, we have developed a series of methods to recycle WCF (Xiong et al. 2012; Sun et al. 2013, 2014; Zhang et al. 2013a). In this study, we investigated the possibility of mechanochemical preparation of CFC from WCF and tested its adsorption capacity for cationic dyes. A self-designed pan-mill type mechanochemical reactor was applied to realize the surface carboxylation of WCF. Derived from the traditional Chinese stone-mill, the innovative pan-mill equipment is efficient in mechanochemical reactions owing to its unique structure (Zhang et al. 2011; Wang et al. 2013). The morphological and

structural development of WCF during the milling process were characterized by scanning electron microscopy (SEM), Fourier transform infrared spectra (FTIR), X-ray diffraction (XRD) analysis, etc. MB and rhodamine 6G (R6G) were chosen as target contaminants to characterize the adsorptive properties of CFC and WCF. The parameters which may affect the adsorption, including concentration of carboxyl groups, initial dye concentration, pH, and temperature, were investigated. The equilibrium data were fitted to Langmuir and Freundlich isotherms and thermodynamic parameters for the present systems were determined based on the isotherm data in order to obtain a better understanding of the adsorption for MB and R6G in this novel adsorbent.

Materials and methods

Materials

Waste cotton fabrics (WCF) were collected from tailoring workshops and used without further purification or bleaching. Analytical grade MB (Chemical formula: $C_{16}H_{18}ClN_3S$, molecular weight: 373.9 g/mol), R6G (Chemical formula: $C_{28}H_{31}N_2O_3Cl$, molecular weight: 479.0 g/mol) and succinic anhydride were commercially obtained from Chengdu Kelong Chemical Plant, China. Deionized water was used throughout the experiment. Standard dye solutions of 1,000 mg/L were prepared as starting solutions and subsequently diluted when necessary. The pH of each solution was adjusted to the required value with diluted or concentrated HCl and NaOH before introducing adsorbent.

Preparation of CFC

Mechanochemical synthesis of carboxylate-functionalized cellulose (CFC) from WCF was performed using the pan-mill type mechanochemical reactor. The details of the pan-mill equipment and operation procedure can be found in our previous publications (Zhang et al. 2011, 2013b). Generally, a mixture of WCF/succinic anhydride with weight ratio of 4:1 was fed into hopper set at the middle of the moving pan. Milled powder was discharged from the brim of the pans. The discharged powder was then collected for the next milling cycle. The whole milling process was controlled at a rotating speed of 60 rpm and at ambient

temperature. The obtained powder was Soxhlet extracted with ethanol for 48 h to ensure thorough removal of residual succinic anhydride for subsequent analysis.

Characterization of CFC

Observations of WCF morphologies before and after mechanochemical modification were performed using a scanning electron microscopy (SEM) (JEOL JSM-5600, Japan) equipment. A thin layer of Pd–Au alloy was coated on the specimen prior to measurement to prevent charging on the surface.

Fourier transform infrared spectroscopy (FTIR) studies were conducted on a Nicolet 560 spectrophotometer (USA). The modified cellulose powder samples were mixed with KBr to produce tablets. The spectra were recorded from 4,000 to 400 cm^{-1} at a resolution of 4 cm^{-1} over 20 scans.

XRD patterns were collected on a Philips Analytical X'Pert X-diffractometer (Philips Co., Netherlands), using Cu-K α radiation ($\lambda = 0.1540\text{ nm}$) at an accelerating voltage of 40 kV and a current of 40 mA. The data were collected from $2\theta = 5^\circ\text{--}50^\circ$ with a step interval of 0.03° . The degree of crystallinity can be relatively expressed by the percentage crystallinity index (%CrI). The equation used to calculate the CrI was described by Segal et al. (1959) in the following form:

$$CrI(\%) = [(I_{200} - I_{am})/I_{200}] \times 100 \quad (1)$$

where I_{200} is the maximum intensity of the 200 reflection and I_{am} corresponds to the minimum intensity located 2θ close to 18° . The average crystal size τ was determined by the Scherrer equation (French and Santiago Cintrón 2013):

$$\tau = K\lambda/(\beta \cos \theta) \quad (2)$$

where K is a constant that depends on the crystal shape (1.0 in this case), λ is the wavelength of the incident beam in the diffraction experiment, β is the full width at half maximum in radians and θ is the position of the peak (half of the plotted 2θ value).

The concentration of carboxyl groups on the modified cellulose was determined by back-titration method. 0.1 g CFC was suspended in 100 mL 0.01 mol/L NaOH aqueous solution for 1 h under constant stirring. After filtration, the excess NaOH was back-titrated with 0.01 mol/L HCl solution. The

concentration of carboxylic functions was calculated via following equation (Zhang et al. 2010a):

$$C_{\text{COOH}} = \left[\frac{(C_{\text{NaOH}} \times V_{\text{NaOH}}) - (C_{\text{HCl}} \times V_{\text{HCl}})}{M_{\text{CFC}}} \right] \quad (3)$$

where C_{NaOH} is the concentration of the NaOH solution (mmol/L), C_{HCl} is the concentration of the HCl solution (mmol/L), V_{NaOH} is the volume of the NaOH solution (L), V_{HCl} is the volume of HCl spent in the titration of the excess base (L) and M_{CFC} is the modified cellulose mass (g).

The pH_{zpc} of the adsorbent is determined by powder addition method (Al-Degs et al. 2006). 0.5 g of CFC was added to 100 mL conical flask containing 50 mL of 0.1 M NaCl solution. Several batches were carried out for various initial solution pH, called pH_i . The pH was adjusted using 0.1 M HCl and 0.1 M NaOH solution. The electrolyte solution with CFC was equilibrated for 24 h. After equilibration, the final pH, marked as pH_f was recorded. Both positive and negative ΔpH ($\text{pH}_i - \text{pH}_f$) values recorded for the CFC are plotted against the pH_i values. The pH at which ΔpH becomes 0 is called pH_{zpc} .

Dye adsorption experiments

The adsorption experiments were carried out in a 250 mL stopper conical flask containing varying amount of MB or R6G solutions and adsorbent dosages. Then the mixtures were agitated in incubated rotary shakers at 60 rpm under a constant temperature for 4 h to ensure equilibrium. The samples were centrifuged and the residual concentration in the supernatant solution was analyzed using a UV/VIS spectrometry (model UV754GD, Shanghai) by monitoring the absorbance changes at a wavelength of maximum absorbance (665 nm for MB and 526 nm for R6G).

The amounts of dyes adsorbed by the CFC were calculated using the following equation:

$$q_e = \frac{(C_o - C_e)V}{W} \quad (4)$$

where q_e (mg/g) is the amount of dye adsorbed by CFC, C_o and C_e (mg/L) are the initial and equilibrium dye concentrations, respectively, V (L) is the initial volume of dye solution, and W (g) is the weight of the CFC. And the removal efficiency (R) is defined as follows:

$$R = 1 - \frac{C_e}{C_o} \quad (5)$$

The effect of pH on the removal efficiency for the dyes was analyzed over the pH range of 2–10. The pH was adjusted by using 0.1 N NaOH and 0.1 N HCl solutions. 0.1 g CFC or WCF was added to several 250 mL conical flasks with 100 mL of 100 mg/L dye solutions. Then, the equilibrium pH and dye concentrations in solutions were determined.

In the dosage studies, adsorption measurements were conducted by mixing various amounts of CFC (0.1–0.5 g) with 100 mL of dye solutions (200 mg/L) in 250 mL conical flasks. The experiments were carried out at the optimal pH of 10 both for MB and R6G.

Adsorption isotherms

Equilibrium data commonly known as adsorption isotherms are basic requirements for the design of adsorption systems. 100 mL of dye solutions of various concentrations ($C_o = 100$ –800 mg/L) were taken in 250 mL flasks. 0.1 g of each CFC was added to the solution and the mixtures were agitated in incubated rotary shakers ($\text{pH} = 10$, $T = 298$, 308 and 303 K). Langmuir and Freundlich equations were used for present work.

Langmuir isotherm (Langmuir 1918), which is applicable for homogenous surface adsorption, is given as:

$$q_e = \frac{q_o K_L C_e}{1 + K_L C_e} \quad (6)$$

where K_L is the Langmuir constant (L/mg) and q_o is the maximum adsorption capacity (mg/g). Equation (6) can be rearranged into linear form:

$$\frac{C_e}{q_e} = \frac{C_e}{q_o} + \frac{1}{q_o K_L} \quad (7)$$

by plotting C_e/q_e versus C_e , the Langmuir constants can be obtained. The essential characteristics of Langmuir isotherm can be expressed by a separation or equilibrium parameter, which is a dimensionless constant defined as:

$$R_L = \frac{1}{1 + K_L C_o} \quad (8)$$

Freundlich isotherm (Freundlich 1936) is used for liquids to describe adsorption on a surface which has heterogeneous energy distribution. It is given as:

$$q_e = K_F C_e^{\frac{1}{n}} \quad (9)$$

K_F and n are Freundlich constants relating to adsorption capacity and adsorption intensity of the adsorbents. By rearranging Eq. (9) we get:

$$\ln q_e = \ln K_F + \frac{1}{n} \ln C_e \quad (10)$$

A plot of $\ln q_e$ against $\ln C_e$ yields a straight line which indicates the conformation of the Freundlich adsorption isotherm. The constants $1/n$ and $\ln K_F$ can be determined from the slope and intercept, respectively. The value of Freundlich constant (n) should lie in the range of 1–10 for favorable adsorption.

Non-linear regression was performed using OriginLab for both Langmuir and Freundlich parameters, Average percent error (APE) and the least-squares correlation coefficient (R^2) values were employed to find out the most suitable isotherm model.

Thermodynamic studies

The thermodynamic parameters such as standard Gibbs free energy changes, standard enthalpy changes and standard entropy changes (ΔG° , ΔH° , ΔS°) have a significant role to define the feasibility, spontaneity and heat change for the adsorption process and can be estimated by the following equations (Khan and Singh 1987; Deniz and Saygideger 2011):

$$\Delta G^\circ = -RT \ln K_C \quad (11)$$

$$\ln K_C = -\frac{\Delta H^\circ}{RT} + \frac{\Delta S^\circ}{R} \quad (12)$$

where K_C is the equilibrium constant (C_s/C_e , C_s is the equilibrium dye concentration on adsorbent), R is the

gas constant and T is the absolute temperature (K). By plotting $\ln K_C$ versus $1/T$, the values of ΔH° and ΔS° can be determined from the slope and intercept, respectively.

Results and discussion

Morphological observation

The SEM images of WCF before (a) and after 5 (b) and 20 (c) cycles of pan-milling together with succinic anhydride are shown in Fig. 1. The entangled cellulose fibers and bundles like ropes with smooth surface are observed in Fig. 1a. After 5 cycles of milling, the original belt-like cellulose fibers began to lose their fibrillar structure and were cut off due to the strong shearing and squeezing forces generated by the pan-mill (Wang et al. 2013). Therefore, the entangled fiber bundles break into small pieces as shown in Fig. 1b. Figure 1c presents that after 20 cycles of milling, the WCF has been transformed into powders with a particle size of 50 μm or less. Furthermore, it acquired a rougher surface and a larger specific area after mechanochemical treatment, which would benefit its adsorption capacity for dyes.

FTIR analysis

The FTIR spectra of raw and carboxylate-functionalized WCF are shown in Fig. 2. The results indicate that the broad stretching vibration absorption band of hydroxyl groups at 3,392 cm^{-1} has hardly changed. This result is different from the acetylation of cellulose in which a reduced intensity of the $-\text{OH}$ stretching

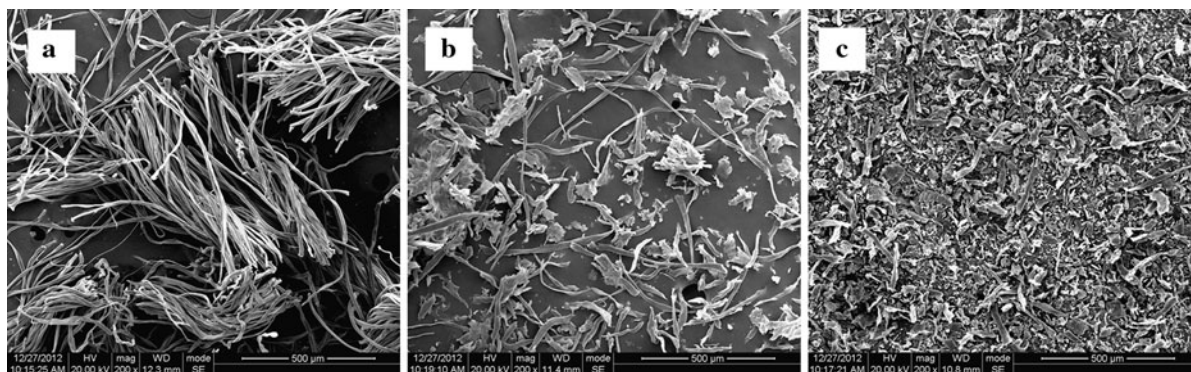


Fig. 1 SEM images of WCF (a) and CFC prepared by 5 cycles (b) and 20 cycles (c) of pan-milling

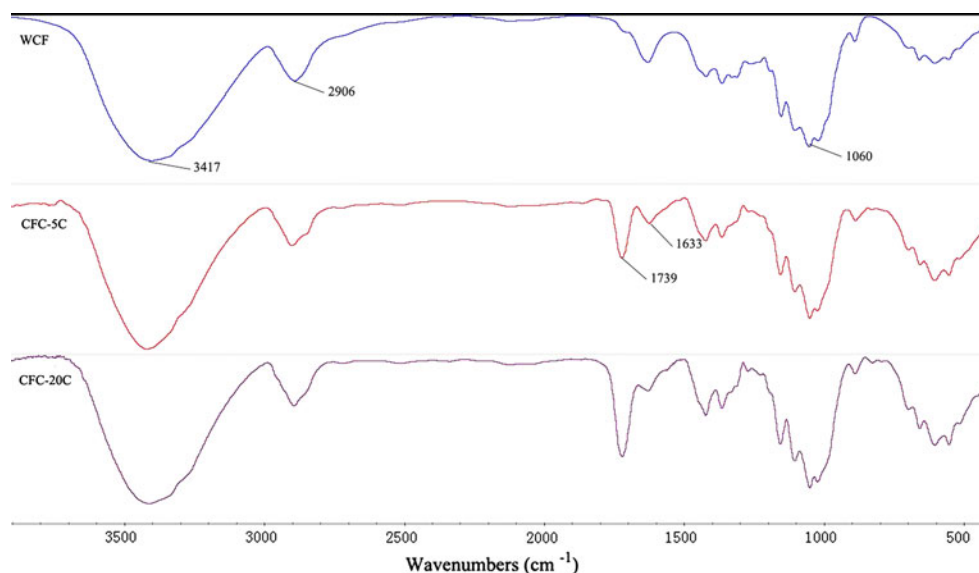


Fig. 2 FTIR spectra of WCF and CFC prepared by 5 cycles and 20 cycles of pan-milling

absorption was observed (Biswas et al. 2007). It is due to the fact that succinic anhydride can hydrolyze to be succinic acid which has two hydroxyl groups, while acetic acid has only one hydroxyl group. The absorption peak around $1,060\text{ cm}^{-1}$ could be ascribed to C-O stretching vibration, which is the symbol of glucose ring. The intensity of this peak is not changed after pan-milling. The most obvious change in the FTIR spectra occurs in the region around $1,739\text{ cm}^{-1}$. In general, the absorption by carbonyl bonds in esters gives a peak at $1,750\text{ cm}^{-1}$, and it exhibits a band at $1,712\text{ cm}^{-1}$ in the carboxylic acids (Jayakumar et al. 2000; Gu and Yang 1998). These two bands are closely overlapped and therefore only one peak centered at $1,739\text{ cm}^{-1}$ was observed as a result, which is along with other similar studies (Gurgel et al. 2008; Li et al. 2009). Moreover, the peak intensity increases with increasing cycles of pan-milling. These results indicate that mechanochemical esterification reaction between cellulose and succinic anhydride occurred during pan-milling.

XRD analysis

The XRD diagrams of raw and carboxylate-functionalized WCF are shown in Fig. 3. It is shown that all the XRD profiles exhibit typical diffraction cellulose I β angles (2θ) around at 14.6° , 16.5° and 22.7° , which are assigned to the diffraction planes of (1–10), (110) and

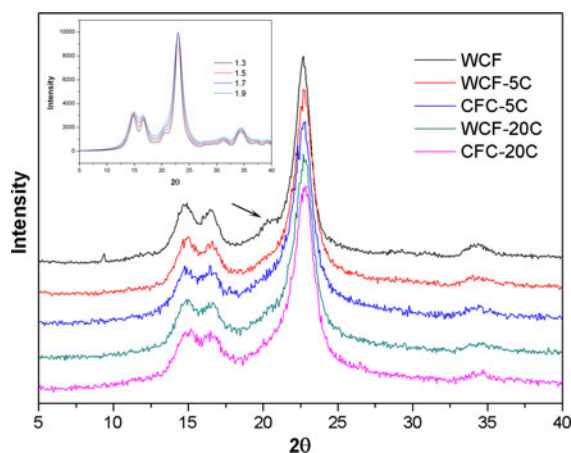


Fig. 3 XRD patterns of WCF and CFC before and after various cycles of pan-milling. Diffraction patterns for cellulose I β calculated for peak widths at half maximum of 1.3° , 1.5° , 1.7° , 1.9° are presented as inset

(200), respectively (Nishiyama et al. 2002). The CrI of WCF obtained by the Segal method decreased from its original 87.4 to 81.3 % after 20 cycles of pan-milling and changed a little during esterification of hydroxyl groups (Table 1), indicating pan-milling activation is the main influence factor to the structure of cellulose. Similar trend was observed in crystal size of WCF which decreased from its original 6.63 to 4.84 nm after activation and esterification. During the pan-milling process, the strong shearing and squeezing forces generated by the pan-mill equipment could break up

Table 1 Segal CI and crystal size of WCF and CFC

Sample	CrI (%)	Crystal size (nm)
WCF	87.4	6.63
WCF-5C	84.9	5.56
CFC-5C	82.0	5.07
WCF-20C	81.3	4.76
CFC-20C	81.9	4.84

the hydrogen bonding network and decrease the crystal size of cellulose. As a result, WCF or CFC experienced more cycles of pan-milling shows lower CrI.

In order to better understand the crystal structure change during pan-milling, some theoretical diffraction patterns which are only based on crystalline material were created using Mercury program, and compared with XRD patterns of WCF and CFC (French 2013; French and Santiago Cintrón 2013). As shown in the inset of Fig. 3, as the input value of pwhm changes from 1.3° to 1.9° (the pwhm of the main (200) peak of WCF and CFC), a series of values of the Segal CI and crystal size for the different pwhm values are obtained. French and Santiago Cintrón (2013) reported a nonlinear relationship between the Segal CI and the crystal size. The values of Segal CI and crystal size of WCF and CFC obtained in this work were in agreement with their calculations. Based on the intensity at about 20.5° assigning to the diffraction planes of (102) and (012) in Fig. 3, there is fairly random orientation of the cellulose fibers in the WCF sample, but preferred orientation in the pan-milled samples, leading to different curve shape in the 18–20° area of the pattern. According to French and Santiago Cintrón, the preferred orientation of cellulose fibers for cellulose I β would increase the Segal CI. However, the Segal CI of all pan-milled samples decreased comparing to that of the pristine WCF sample, indicating pan-milling treatment could decrease the crystal size effectively. Thus the mechanism of pan-milling induced surface-esterification between cellulose and succinic anhydride could be described as follows. Pan-milling caused a size reduction of the crystals of cellulose, making breakage of inter- and intramolecular hydrogen bonds which could produce a large number of free –OH groups at the surface of cellulose powder. The resultant –OH groups at the cellulose surface were activated, and could form acyl bond with succinic anhydride during pan-milling.

Effect of concentration of carboxyl groups

FTIR studies confirmed the mechanochemical esterification reactions between cellulose and succinic anhydride. It is important to investigate the concentration of substituted groups of the prepared CFC. Figure 4 shows the effect of cycles of pan-milling on the carboxylic end group concentration of the modified cellulose as well as dye adsorption capacity for MB and R6G. The concentration of carboxyl groups climbs to 1.34 mmol/g after only 2 cycles of milling, indicating that the surface-acetylation of cellulose during pan-milling was fast and effective. The carboxyl content of the modified cellulose increases with the increase of cycles of pan-milling. The maximum value is obtained after 20 cycles of milling and reaches 2.14 mmol/g. Júnior et al. (2007) reported a concentration of 3.83 mmol/g for carboxylate-functionalized sugarcane bagasse based on chemical modifications in solvent. However, the dosage of succinic anhydride for their system is much higher than that of ours. If a larger amount of succinic anhydride was used in the pan-milling process, a higher concentration of carboxyl groups could be expected. Compared with raw WCF, the adsorption performance of CFC is closely related to its surface carboxyl groups. As shown in Fig. 4, the dye adsorption capacity of CFC for both dyes increases with the increase of the concentration of carboxyl groups and reaches a maximum after 10 cycles of milling. According to the previous analysis (as shown in Fig. 3; Table 1), the changes of CrI and carboxyl content of CFC are rapid at the early stage of the pan-milling process. In order to develop an industrially scalable method, we chose the CFC prepared through 5 cycles of pan-milling as the adsorbent for further adsorption studies.

Effect of pH

One of the important factors that affect the adsorption efficiency is pH. The effect of pH on the adsorption efficiency of CFC was studied by varying pH from 2 to 10 (with the initial dye concentration of 100 mg/L). As shown in Fig. 5, raw WCF has very low adsorption capacity for both two dyes, MB and R6G, at any pH value. This result is quite different from other similar adsorbents (Salleh et al. 2011), which have relatively higher adsorption capacities even without modification. This is because the WCF was dyed once with one or more kinds of dyes during the clothing production

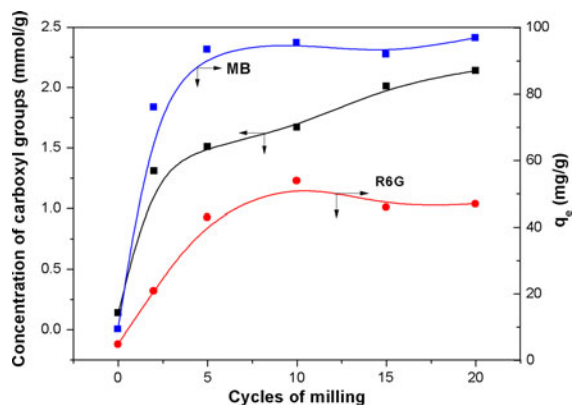
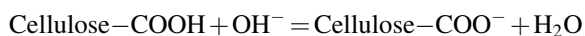
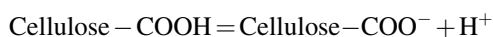


Fig. 4 Effect of concentration of carboxyl groups on the adsorption capacity of CFC for MB and R6G ($\text{pH}=10$, $C_0=100$ mg/L, adsorbent dosage=0.1 g)

process. On the contrary, the modified cellulose shows much higher adsorption efficiency than that of raw WCF due to the carboxylate-functionalization. The maximum removal efficiency was 93.5 % for MB at pH 10 and adsorbent dosage 0.1 g. The adsorption efficiency of the modified cellulose increases with the increase of solution pH. It could be explained on the basis of pH zero point charge (pH_{zpc}). The pH_{zpc} of CFC (Fig. 5) was found to be 4.45. Cationic adsorption on any adsorbent will be favorable at $\text{pH} > \text{pH}_{\text{zpc}}$. The surface charge of the modified cellulose is influenced by the pH of its surrounding environment (Janaki et al. 2013). By either losing or gaining protons (H^+), it can become more negatively or more positively charged. At $\text{pH} < \text{pH}_{\text{zpc}}$ (=4.45), protonation of the carboxyl groups occurred. Thus, repulsive force occurred between the dye cations and the adsorbent surface. In addition, at lower pH, the concentrations of H^+ are high. They competed with the positively charged MB and R6G cations for vacant adsorption sites. Thus, the adsorption efficiency is very low at low pH. The reverse situation occurs at $\text{pH} > \text{pH}_{\text{zpc}}$, the surface of the modified cellulose may get negatively charged due to adsorption of OH^- , and the carboxyl groups of the modified cellulose may get deprotonated to produce negatively charged adsorption sites. The equations are as follows:



Thus at high pH, the adsorption process is highly favored through the electrostatic forces of attraction.

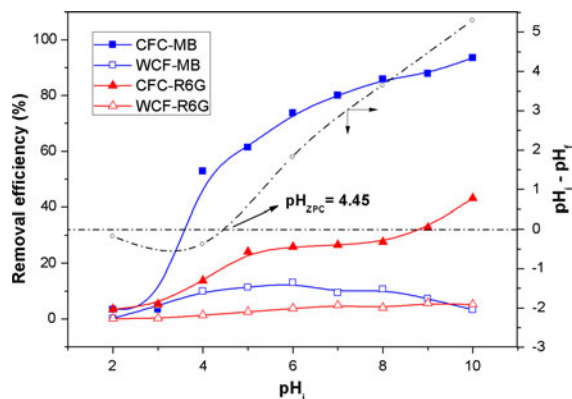


Fig. 5 Effect of initial pH on the removal efficiency of CFC for MB and R6G ($C_0=100$ mg/L, adsorbent dosage=0.1 g)

Since the dye removal showed higher efficiency at high pH, $\text{pH} = 10$ was selected for further experiments.

Effect of adsorbent dosage

Figure 6 shows the effect of adsorbent dosage on the removal of MB and R6G (with the initial dye concentration of 200 mg/L). The removal percentage of the two dyes increases with the increase of adsorbent dosage. This can be attributed to the increased adsorbent surface area and availability of more adsorption sites resulting from the increase of adsorbent dosage. However, Specific dye uptake (q_e) decreased significantly when the adsorbent dosage was increased from 0.1 to 0.5 g. This is due to the fact that the active sites could be effectively utilized when the adsorbent dosage was low (i.e., low adsorbent/adsorbate ratio). When the adsorbent dosage is higher (high adsorbent/adsorbate ratio) it is more likely that a significant portion of the available active sites remain uncovered, which leads to a lower q_e (Ponnusami et al. 2008).

Adsorption isotherms

The adsorption isotherm indicates how the dye molecules distribute between the liquid phase and the solid phase when the adsorption process reaches an equilibrium state. The Langmuir and Freundlich are the most frequently employed models to describe the experimental data of adsorption isotherms. In this study, the adsorption of MB and R6G onto CFC was

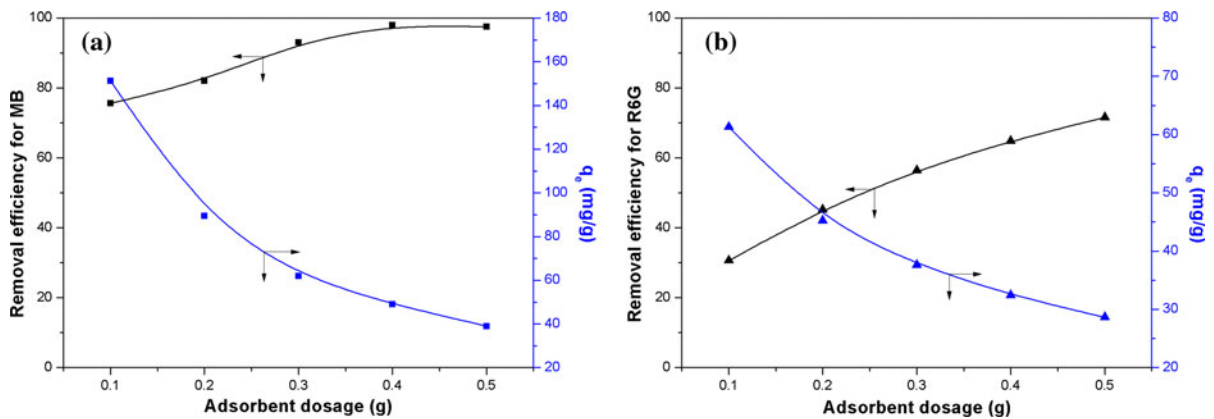


Fig. 6 Effect of adsorbent dosage on the removal efficiency of CFC for MB (a) and R6G (b)(pH=10, $C_o=200$ mg/L)

Table 2 Adsorption isotherm constants for the adsorption of MB and R6G onto CFC at various temperatures

Isotherm models	MB			R6G		
	298 K	308 K	318 K	298 K	308 K	318 K
Langmuir						
$q_{o,exp}$ (mg/g)	185.63	163.31	144.69	118.21	96.48	76.74
q_o (mg/g)	183.22	170.10	151.16	152.46	113.15	84.16
K_L (L/mg)	11.7×10^{-2}	5.71×10^{-2}	4.56×10^{-2}	5.84×10^{-3}	8.86×10^{-3}	12.8×10^{-3}
R_L ($C_o = 800$ mg/L)	1.06×10^{-2}	2.14×10^{-2}	2.67×10^{-2}	17.6×10^{-2}	12.4×10^{-2}	8.90×10^{-2}
R^2	0.963	0.993	0.997	0.956	0.979	0.963
APE (%)	2.84	4.17	4.53	4.73	5.33	4.20
Freundlich						
$1/n$	0.130	0.136	0.146	0.400	0.312	0.251
K_F ((mg/g) (L/mg) $^{1/n}$)	84.09	71.37	59.20	9.34	13.11	15.16
R^2	0.873	0.694	0.735	0.908	0.835	0.877
APE (%)	6.80	9.16	7.86	7.62	4.31	8.70

studied under three temperatures (25, 35 and 45 °C), pH = 10 and different initial dye concentration (100–800 mg/L). Isotherm parameters determined by non-linear regression according to Eqs. (6) and Eq. (9) are presented in Table 2. The data fits well with the Langmuir isotherms yielding high correlation coefficients values ($R^2 > 0.95$) and low average percent error for both dyes (Giménez-Martín et al. 2009). On the contrary, it is found that the Freundlich isotherms model with much lower R^2 values cannot be able to describe the adsorption process accurately. The Freundlich constants ($1/n$) are below 1, which also indicates normal Langmuir isotherms (Zhang et al. 2010b). Conformation of the experimental data into Langmuir isotherm model indicates the homogeneous

nature of adsorbent surface, which is an evidence that esterification only occurs homogeneously on the surface of the WCF during pan-milling. The value of dimensionless separation parameter, R_L , indicating the shape of isotherm as follows: $R_L > 1$, unfavorable; $R_L = 1$, linear; $0 < R_L < 1$, favorable; $R_L = 0$, irreversible. In this study, all R_L values are found to be in the range of 0–1, suggesting favorable adsorption process.

Figure 7 shows a typical comparison of predicted and experimental equilibrium data at 25 °C for MB (a) and R6G (b). The adsorption capacity (q_e) increases with the equilibrium concentration of C_e in solution for both dyes. The maximum adsorption capacity of CFC obtained from the experiments is

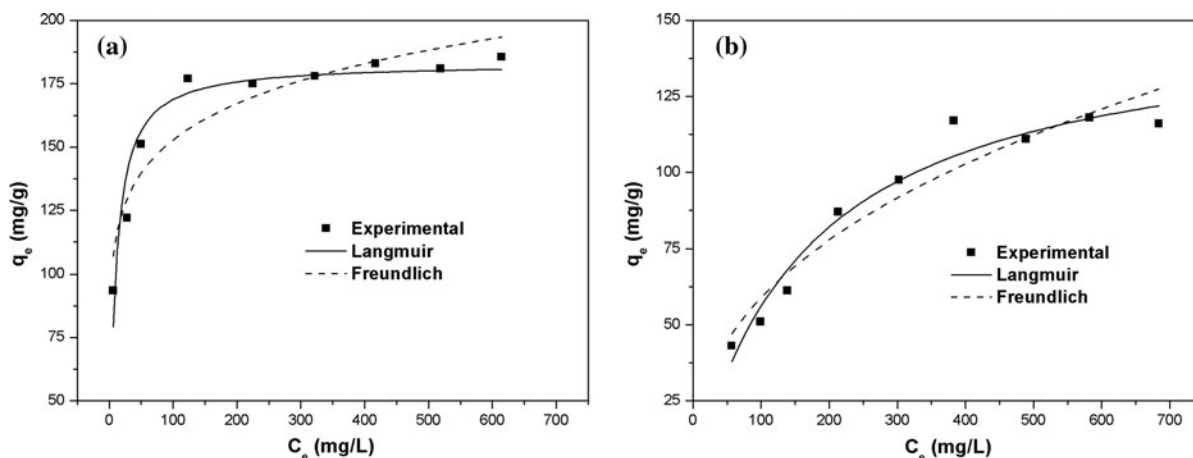


Fig. 7 Non-linear regression of adsorption isotherms of MB (a) and R6G (b) onto CFC at 25 °C (pH=10, $C_0=100\text{--}800$ mg/L, adsorbent dosage=0.1 g)

found to be 185.63 mg/g for MB and 118.21 mg/g for R6G, respectively. The maximum adsorption capacity for MB is significant comparing to other low-cost adsorbents such as modified sawdust (32.3 mg/g) (De and Basu 1998), garlic peel (82.64 mg/g) (Hameed and Ahmad 2009), rice husk (40.59 mg/g) (Vadivelan and Kumar 2005). The maximum adsorption capacity values of adsorbents are usually below 200 mg/g (Rafatullaha et al. 2010). The values measured in this study are higher than most of the values reported in previous studies, indicating an attractive application of CFC in terms of dye removal from wastewater.

Thermodynamic studies

The thermodynamic parameters were calculated according to Eqs. (11) and (12) and the results are presented in Table 3. The negative value of ΔH° (-26.48 kJ/mol for MB and -42.16 kJ/mol for R6G) suggests that the process is exothermic in nature while the positive value of ΔS° (75.19 J/(K mol) for MB and 145.71 J/(K mol) for R6G) shows an increase disorder at the interface between solid and liquid during the adsorption (Deniz and Saygideger 2011). The negative ΔG° values for MB decrease from -4.16 to -2.67 kJ/mol in the temperature range of 298–318 K, suggesting the adsorption is spontaneous and in accordance with the exothermic nature. Generally, a value of ΔG° between 0 and -20 kJ/mol is consistent with electrostatic interaction between adsorption sites and the adsorbing ion (physical adsorption), indicating that the adsorption for MB in this study is a typical

Table 3 Thermodynamic parameters for the adsorption of MB and R6G onto CFC

Dyes	Temp. (K)	ΔG° (kJ/mol)	ΔH° (kJ/mol)	ΔS° (J/(K mol))
MB	298	-4.16	-26.48	75.19
	308	-3.15		
	318	-2.67		
R6G	298	1.13	-42.16	145.71
	308	2.99		
	318	4.03		

physical adsorption process (Fernandes et al. 2010). However, the positive sign of ΔG° for R6G implies that the adsorption by CFC is non-spontaneous. This difference can be attributed to the molecular size effect that dyes with larger-sized molecules (such as R6G in this study) are more difficult to be adsorbed compared to dyes with smaller molecules (Mui et al. 2010).

Conclusions

We have demonstrated a facile and environmentally friendly solvent-free approach to prepare adsorbents from waste cotton fabrics. WCF was reacted with succinic anhydride through solvent-free mechanochemical pan-milling at ambient temperature. In such reaction, esterification is primarily due to mechanochemical formation of reactive hydroxyl groups on the surface of cellulose. The resulting carboxylate-functionalized cellulose showed excellent adsorption

capacities for cationic dyes in aqueous solutions. Because the concepts of the process are simple and the use of waste cotton fabrics can alleviate the environmental pollution from waste textiles, the suggested route is suitable for industrial-scale production and may be extended to the synthesis of other cellulose derivatives from waste fabrics.

Acknowledgments The authors would like to thank the National Science Foundation of China (51203105) and National High Technology Research and Development Program (863 Program, SS2012AA062613) for financial support.

References

- Al-Degs YS, El-Barghouthi MI, Issa AA, Khraisheh MA, Walker GM (2006) Sorption of Zn (II), Pb(II), and Co (II) using natural sorbents: equilibrium and kinetic studies. *Water Res* 40:2645–2658
- Annadurai G, Juang R, Lee D (2002) Use of cellulose-based wastes for adsorption of dyes from aqueous solutions. *J Hazard Mater B92*:263–274
- Biswas A, Selling G, Appell M, Woods KK, Willett JL, Buchanan CM (2007) Iodine catalyzed esterification of cellulose using reduced levels of solvent. *Carbohydr Polym* 68:555–560
- Bulut Y, Aydin HA (2006) Kinetics and thermodynamics study of methylene blue adsorption on wheat shells. *Desalination* 194:259–267
- Chao AC, Shyu SS, Lin YC, Mi FL (2004) Enzymatic grafting of carboxyl groups on to chitosan—to confer on chitosan the property of a cationic dye adsorbent. *Bioresour Technol* 91:157–162
- De DS, Basu JK (1998) Adsorption of methylene blue on to a low cost adsorbent developed from sawdust. *Ind J Environ Protec* 19:416–421
- Demirbas A (2009) Agricultural based activated carbons for the removal of dyes from aqueous solutions: a review. *J Hazard Mater* 167:1–9
- Deniz F, Saygideger SD (2011) Removal of a hazardous azo dye (Basic Red 46) from aqueous solution by princess tree leaf. *Desalination* 268:6–11
- Fernandes AN, Almeida CAP, Debacher NA, Sierra MMDS (2010) Isotherm and thermodynamic data of adsorption of methylene blue from aqueous solution onto peat. *J Mol Struct* 982:62–65
- French AD (2013) Idealized powder diffraction patterns for cellulose polymorphs. *Cellulose*. doi:10.1007/s10570-013-0030-4
- French AD, Santiago Cintrón M (2013) Cellulose polymorphy, crystallite size, and the Segal crystallinity index. *Cellulose* 20:583–588
- Freundlich H (1936) Adsorptionstechnik. *J Phys Chem* 40:857–858
- Giménez-Martín E, López-Andrade M, Ontiveros-Ortega A, Espinosa-Jiménez M (2009) Adsorption of chlorhexidine onto cellulosic fibers. *Cellulose* 16:467–479
- Gong R, Sun Y, Chen J, Liu H, Yang C (2005) Effect of chemical modification on dye adsorption capacity of peanut hull. *Dyes Pigm* 67:175–181
- Gu X, Yang CQ (1998) FT-IR and FT-Raman spectroscopy study of the cyclic anhydride intermediates for esterification of cellulose: I. Formation of anhydrides without a catalyst. *Res Chem Intermed* 24:979–996
- Gurgel LVA, Júnior OK, Gil RPDF, Gil LF (2008) Adsorption of Cu(II), Cd(II), and Pb(II) from aqueous single metal solutions by cellulose and mercerized cellulose chemically modified with succinic anhydride. *Bioresour Technol* 99:3077–3083
- Hameed BH, Ahmad AA (2009) Batch adsorption of methylene blue from aqueous solution by garlic peel, an agricultural waste biomass. *J Hazard Mater* 164:870–875
- Janaki V, Vijayaraghavan K, Oh BT, Ramasamy AK, Kamala-Kannan S (2013) Synthesis, characterization and application of cellulose/polyaniline nanocomposite for the treatment of simulated textile effluent. *Cellulose*. doi:10.1007/s10570-013-9910-x
- Jayakumar R, Balaji R, Nanjundan S (2000) Studies on copolymers of 2-(Nphthalimido)ethyl methacrylate with methyl methacrylate. *Eur Polym J* 36:1659–1666
- Júnior OK, Gurgel LVA, Melo JCP, Botaro VR, Melo TMS, Gil RPDF, Gil LF (2007) Adsorption of heavy metal ion from aqueous single metal solution by chemically modified sugarcane bagasse. *Bioresour Technol* 98:1291–1297
- Khan AA, Singh RP (1987) Adsorption thermodynamics of carbolfuran on Sn (IV) arsenosilicate in H⁺, Na⁺ and Ca²⁺ forms. *Colloids Surf* 24:33–42
- Langmuir I (1918) The adsorption of gases on plan surfaces of glass, mica and platinum. *J Am Chem Soc* 40:1361–1403
- Li WY, Jin AX, Liu CF, Sun RC, Zhang AP, Kennedy JF (2009) Homogeneous modification of cellulose with succinic anhydride in ionic liquid using 4-dimethylaminopyridine as a catalyst. *Carbohydr Polym* 78:389–395
- Mane VS, Mall ID, Srivastava VC (2007) Use of bagasse fly ash as an adsorbent for the removal of brilliant green dye from aqueous solution. *Dyes Pigm* 73:269–278
- Mao YH, Guan Y, Zheng QK, Feng XN, Wang XX (2011) Adsorption thermodynamic and kinetic of disperse dye on cotton fiber modified with tolylene diisocyanate derivative. *Cellulose* 18:271–279
- Miranda R, Sosa-Blanco C, Bustos-Martinez D, Vasile C (2007) Pyrolysis of textile wastes: I. Kinetics and yields. *J Anal Appl Pyrol* 80:489–495
- Mui ELK, Cheung WH, Valix M, McKay G (2010) Dye adsorption onto char from bamboo. *J Hazard Mater* 177:1001–1005
- Nandi BK, Goswami A, Purkait MK (2009) Removal of cationic dyes from aqueous solutions by kaolin: kinetic and equilibrium studies. *Appl Clay Sci* 42:583–590
- Nishiyama Y, Langan P, Chanzy H (2002) Crystal structure and hydrogen-bonding system in cellulose I β from synchrotron X-ray and neutron diffraction. *J Am Chem Soc* 124:9074–9082
- Ponnusami V, Vikram S, Srivastava SN (2008) Guava (*Psidium guajava*) leaf powder: novel adsorbent for removal of methylene blue from aqueous solutions. *J Hazard Mater* 152:276–286

- Rafatullaha M, Sulaimana O, Hashima R, Ahmad A (2010) Adsorption of methylene blue on low-cost adsorbents: a review. *J Hazard Mater* 177:70–80
- Saliba R, Gauthier H, Gauthier R, Petit-Ramel M (2002) The use of amidoximated cellulose for the removal of metal ions and dyes from waste waters. *Cellulose* 9:183–191
- Salleh MAM, Mahmouda DK, Karima WAWA, Idris A (2011) Cationic and anionic dye adsorption by agricultural solid wastes: a comprehensive review. *Desalination* 280:1–13
- Segal L, Creely JJ, Martin AE, Conrad CM (1959) An empirical method for estimating the degree of crystallinity of native cellulose using the X-ray diffractometer. *Textile Res J* 29:786–794
- Sun X, Lu C, Zhang W, Tian D, Zhang X (2013) Acetone-soluble cellulose acetate extracted from waste blended fabrics via ionic liquid catalyzed acetylation. *Carbohydr Polym* 98:405–411
- Sun X, Lu C, Liu Y, Zhang W, Zhang X (2014) Melt-processed poly (vinyl alcohol) composites filled with microcrystalline cellulose from waste cotton fabrics. *Carbohydr Polym* 101:642–649
- Uddin MT, Islam MA, Mahmud S, Rukanuzzaman M (2009) Adsorptive removal of methylene blue by tea waste. *J Hazard Mater* 164:53–60
- Vadivelan V, Kumar KV (2005) Equilibrium, kinetics, mechanism, and process design for the sorption of methylene blue onto rice husk. *J Colloid Interf Sci* 286:90–100
- Wang M, Zhang X, Zhang W, Tian D, Lu C (2013) Thermoplastic polyurethane composites prepared from mechanochemically activated waste cotton fabric and reclaimed polyurethane foam. *J Appl Polym Sci* 128:3555–3563
- Xiong R, Zhang X, Tian D, Zhou Z, Lu C (2012) Comparing microcrystalline with spherical nanocrystalline cellulose from waste cotton fabrics. *Cellulose* 19:1189–1198
- Xu X, Gao BY, Yue QY, Zhong QQ (2010) Preparation and utilization of wheat straw bearing amine groups for the sorption of acid and reactive dyes from aqueous solutions. *J Hazard Mater* 182:1–9
- Yang F, Bai X, Xu B, Guo H (2013) Triphenylene-modified chitosan: novel high efficient sorbent for cationic and anionic dyes. *Cellulose* 20:895–906
- Zhang W, Li C, Liang M, Geng Y, Lu C (2010a) Preparation of carboxylate-functionalized cellulose via solvent-free mechanochemistry and its characterization as a biosorbent for removal of Pb^{2+} from aqueous solution. *J Hazard Mater* 181:468–473
- Zhang Z, Zhang Z, Fernández Y, Menéndez JA, Niu H, Peng J, Guo S (2010b) Adsorption isotherms and kinetics of methylene blue on a low-cost adsorbent recovered from a spent catalyst of vinyl acetate synthesis. *Appl Surf Sci* 256:2569–2576
- Zhang X, Lu C, Zheng Q, Liang M (2011) An environmental friendly approach for recycling of post-vulcanized fluoro-elastomer scraps through high-shear mechanical milling. *Polym Advan Technol* 22:2104–2109
- Zhang X, Zhang W, Tian D, Zhou Z, Lu C (2013a) A new application of ionic liquids for heterogeneously catalyzed acetylation of cellulose under solvent-free conditions. *RSC Adv* 3:7722–7725
- Zhang X, Tian D, Zhang W, Zhu J, Lu C (2013b) Morphology, foaming rheology and physical properties of ethylene-propylene diene rubber/ground tyre rubber (GTR) composite foams: effect of mechanochemical devulcanisation of GTR. *Prog Rubber Plast Re* 29:81–98